This is a **preprint** version of the article. It has not been peer reviewed. The definitive, peer-reviewed published version is:

Aslanov V.S., Ledkov A.S., Skyhook in Phobos's QSO: Preliminary design, tether deployment, and rover delivery, Acta Astronautica, Vol. 252, 2027, Pages 288–296, https://doi.org/10.1016/j.actaastro.2026.11.029.

Skyhook in Phobos's QSO: preliminary design, tether deployment, and rover delivery

Vladimir S. Aslanov [1], Alexander S. Ledkov [2]

Samara National Research University, 34, Moscovskoe shosse, Samara 443086, Russia

Abstract

This study presents a preliminary mission design for exploring the Phobos surface using a rover delivered by a tether system from a quasi-satellite orbit. Surface cargo exchange is assumed to be performed via a variable-length tether system capable of rotation. The proposed concept adapts the Skyhook design to the restricted three-body problem, where the orbital motion of the tether system is synchronised with its rotation about the center of mass to achieve zero relative surface velocity at the lowest point of the tether trajectory. The primary objective is to verify the physical feasibility of this approach for low-altitude quasi-satellite orbits within the restricted three-body problem framework. A mathematical model describing the planar motion of a tether system with a massless tether is developed using Lagrange's formalism. Numerical simulations are performed to identify system parameters and initial conditions that allow deployment, thruster-induced spin-up, and zero-relative-velocity contact with the Phobos surface. The present analysis is not concerned with optimality; it merely demonstrates that at least one feasible motion scenario exists, thereby confirming the viability of the proposed mission concept.

Keywords: skyhook, space tether; length control; deployment; spin-up control; Phobos; quasi-satellite orbit; restricted three-body problem; mission design

1. Introduction

The scientific community has long been interested in Phobos, one of the moons of Mars. This moon is particularly valuable because it can reveal new insights

[1] E-mail address: aslanov_vs@mail.ru. Website: http://aslanov.ssau.ru
[2] E-mail address: ledkov@inbox.ru. Website: http://www.ledkov.com

This is a **preprint** version of the article. It has not been peer reviewed. The definitive, peer-reviewed published version is:

Aslanov V.S., Ledkov A.S., Skyhook in Phobos's QSO: Preliminary design, tether deployment, and rover delivery, Acta Astronautica, Vol. 252, 2027, Pages 288–296, https://doi.org/10.1016/j.actaastro.2026.11.029.

into the history of the Solar System, the formation of its planets, and the evolution of the surface and atmosphere of Mars [1]. In 1988, the USSR launched the Phobos program. The Phobos-2 spacecraft obtained the first images of Phobos but was lost during its final approach without deploying its landers [2]. Subsequently, several Mars orbiters, namely Mars Global Surveyor [3], Mars Express [4], and Mars Reconnaissance Orbiter [5], have imaged Phobos at various times. Of particular interest was the Russian Phobos-Grunt mission [6], which aimed to return soil samples from the surface of Phobos to Earth. Unfortunately, the spacecraft failed to leave Earth's parking orbit and burned up in the atmosphere. Active preparations are currently underway for the Martian Moons eXploration (MMX) mission [7], which plans to deploy a rover on the surface of Phobos, land an orbital module, and return samples to Earth. Among the proposed but unrealised projects, the NASA “Hall” mission, which was rejected due to high costs [8], and the Phobos L1 Operational Tether Experiment (PHLOTE) [9], which proposed using tether systems for Phobos exploration, are worth noting. The concept of using tether systems for Phobos studies has been further developed in [10,11]. The present work offers another option for developing the idea of using tether systems in a Phobos exploration mission.

Recent literature has examined numerous tether-based projects for in-orbit transportation. The use of tethers allows propellant consumption to be eliminated or significantly reduced. A fairly comprehensive review of possible tether applications and the associated scientific challenges is provided in [12]. To address transport problems, various types of space tether systems can be employed. Momentum-exchange tethers involve capturing a payload with a tether system and then releasing it when its angular momentum has changed as required [13]. The redistribution of angular momentum between the bodies connected by the tether occurs as the tether orientation changes. Variable-length space tether systems allow for such redistribution by varying the tether length [14]. Controlling the tether length allows the tether system to oscillate and provides an additional change in the velocity increment upon payload separation from the tether [15]. Space elevators attached to

This is a **preprint** version of the article. It has not been peer reviewed. The definitive, peer-reviewed published version is:

Aslanov V.S., Ledkov A.S., Skyhook in Phobos's QSO: Preliminary design, tether deployment, and rover delivery, Acta Astronautica, Vol. 252, 2027, Pages 288–296, https://doi.org/10.1016/j.actaastro.2026.11.029.

the surface of a planet [16] or moon [17,18], as well as partial space elevators [19,20], allow cargo to be moved from one end of a tether system to the other using electrical energy. Electrodynamic tether systems [21,22] utilise the Earth's electromagnetic field to accelerate or decelerate the tether system. It is also worth noting the potential of using space tether systems to study planetary satellites, in particular, the Moon [23], Phobos [9], and Io [24].

This paper discusses a development of the Skyhook concept [25], which is a rotating momentum-exchange tether system whose rotation is synchronised with the orbital motion such that, at the moment of docking, the lower end of the tether has a significantly lower relative velocity than the orbital velocity. This would allow light rockets or even supersonic aircraft to deliver cargo into orbit. It should be noted that the term "Sky-Hook" was also used to describe a space elevator attached to the surface of a planet [26]. In study [27], the authors propose using two skyhooks, which are rotating space tether systems in low Earth and intermediate orbits, to reduce the cost of flights to the Moon and Mars. Moravec's paper [25] proposes using a lunar skyhook to perform exchange operations with the lunar surface. According to this concept, the tether system's orbital rotation and its relative rotation are synchronised so that the end of the tether touches the Moon with zero velocity relative to the surface. A development of Moravec's skyhook idea is the Lunavator [28], a three-body space tether system with a central station that can regulate angular velocity of the system while moving along the tether, ensuring that the tether tip has zero velocity upon touching the lunar surface. This allows for the use of non-circular orbits and shorter tether lengths. The concept proposed in this study differs from Moravec's Skyhook and the Lunavator in that: 1) a tether system consisting of two bodies rather than three is used; 2) the tether has variable length; and 3) the motion of the system's centre of mass does not follow a Keplerian orbit, but rather a quasi-satellite orbit within the framework of the restricted circular three-body problem.

This is a **preprint** version of the article. It has not been peer reviewed. The definitive, peer-reviewed published version is:

Aslanov V.S., Ledkov A.S., Skyhook in Phobos's QSO: Preliminary design, tether deployment, and rover delivery, Acta Astronautica, Vol. 252, 2027, Pages 288–296, https://doi.org/10.1016/j.actaastro.2026.11.029.

This study aims to develop a transport concept for Phobos surface exploration using a variable-length rotating tether system to enable transfers between a quasi-satellite orbit and the surface, and to verify its physical feasibility. The proposed approach extends the Skyhook concept to the restricted three-body problem. The remainder of the paper is organised as follows. Section 2 describes the concept of a Phobos surface exploration mission, including the phases of rover delivery to the surface and sample collection, both performed using a rotating tether system. The equations of motion are derived in Section 3 using Lagrange's equations of the second kind; an analytical tether deployment law is also proposed there. Section 4 presents the results of numerical simulations confirming the feasibility of the proposed concept. Section 5 provides the main conclusions of the study.

2. Mission concept

This study proposes a mission to explore the surface of Phobos. An orbiter spacecraft is delivered from Earth to Phobos and inserted into a quasi-satellite orbit that passes within a few kilometres of Phobos's surface at its closest approach. This orbit was chosen because, owing to Phobos's small mass, conventional Keplerian elliptical orbits are not feasible, since they would intersect the surface. Surface exploration is performed by a rover, which, unlike in the MMX mission, is delivered to the surface using a tether. The rover has a mass of approximately 300 kg and is designed to carry out both autonomous soil investigations and sample collection for return to Earth. A key feature of the proposed architecture is the use of a rotating, variable-length tether system to deliver the rover to the surface and later retrieve a container with the collected samples back to the orbiter. The orbiter itself does not land on Phobos.

The mission can be divided into five phases (Fig. 1): (1) the transfer from Earth to a quasi-satellite orbit, (2) delivery of the rover to the surface, (3) preparation of samples for return by the rover, (4) lifting of the collected soil from the surface to the orbiter, and (5) the return flight of the module to Earth. In this study, we focus

This is a **preprint** version of the article. It has not been peer reviewed. The definitive, peer-reviewed published version is:

Aslanov V.S., Ledkov A.S., Skyhook in Phobos's QSO: Preliminary design, tether deployment, and rover delivery, Acta Astronautica, Vol. 252, 2027, Pages 288–296, https://doi.org/10.1016/j.actaastro.2026.11.029.

on phases 2 and 4, which involve a space tether system. A brief description of the stages of these phases is given in Table 1.

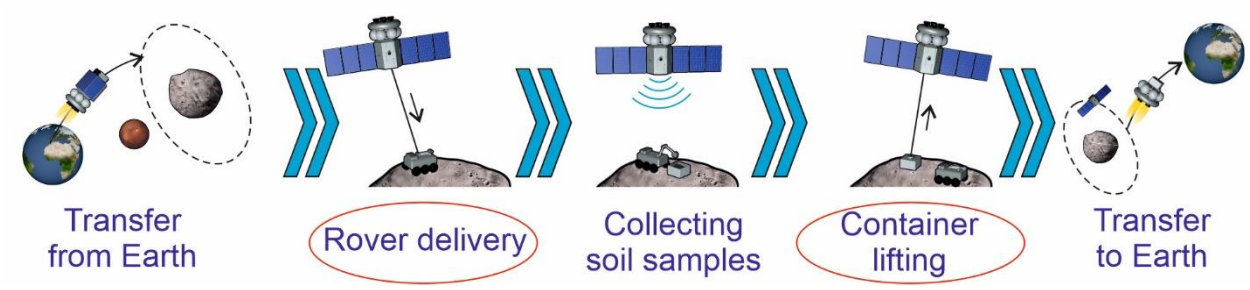


Fig. 1 – The mission phases.

The phase 2 of the mission is shown in Fig. 2. Once the orbiter is in its quasi-satellite orbit, it deploys a tether with the rover attached to its end. The system then switches to rotation mode. Following this, the rotation-control phase begins, the goal of which is to synchronise the system's orbital motion with its spin about the centre of mass. This synchronisation ensures that the tip of the tether has zero velocity relative to the surface of Phobos at the moment of contact. Upon contact, the rover detaches from the tether end. The deployment mechanism must provide some slack in the tether; otherwise, a taut tether will cause a recoil effect upon release. After the rover detaches, the centre of mass of the remaining tether system shifts to a new position. The orbiter's return to a stable quasi-satellite orbit after detachment is achieved by adjusting the length of the tether.

This is a **preprint** version of the article. It has not been peer reviewed. The definitive, peer-reviewed published version is:

Aslanov V.S., Ledkov A.S., Skyhook in Phobos's QSO: Preliminary design, tether deployment, and rover delivery, Acta Astronautica, Vol. 252, 2027, Pages 288–296, https://doi.org/10.1016/j.actaastro.2026.11.029.

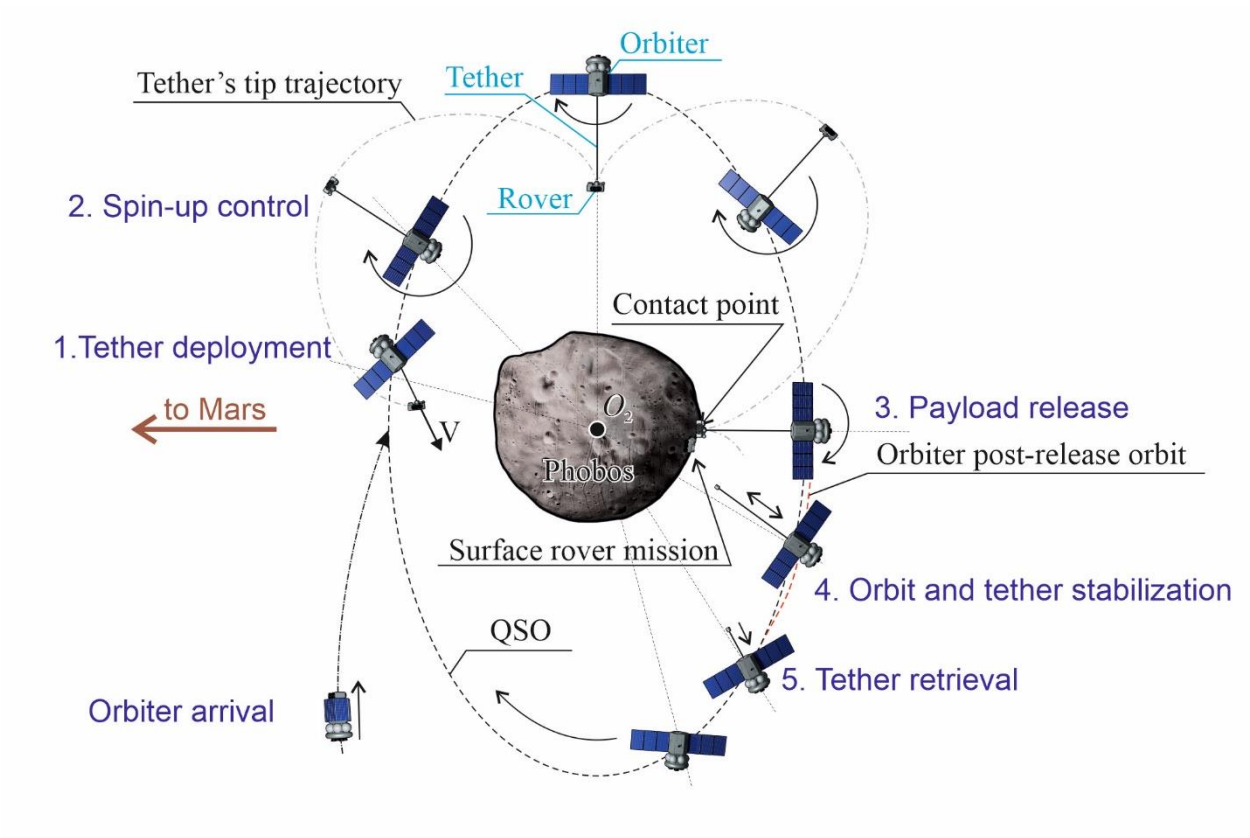


Fig. 2 – Phase of the rover delivery to the surface.

The sample lifting phase is shown on Fig. 3. It follows the same operational sequence. The rover fills the container with soil and returns it to the designated contact point. The tether system deploys again and synchronises its rotation with the orbiter's motion. The end of the tether hooks the container at the contact point. At the moment of container capture, the tether system's centre of mass approaches Phobos's centre of mass. To compensate for this disturbance, the length of the tether must be changes. Capture can be accomplished directly using a hook that engages a wire ring on the container. Alternatively, the container could deploy a net that is caught by the hook. After capture, the tether system retracts, drawing the container back to the orbiter. Once aboard, the container is placed into the return module, which then detaches and, using its thrusters, is inserted onto a trajectory towards Earth.

This is a **preprint** version of the article. It has not been peer reviewed. The definitive, peer-reviewed published version is:

Aslanov V.S., Ledkov A.S., Skyhook in Phobos's QSO: Preliminary design, tether deployment, and rover delivery, Acta Astronautica, Vol. 252, 2027, Pages 288–296, https://doi.org/10.1016/j.actaastro.2026.11.029.

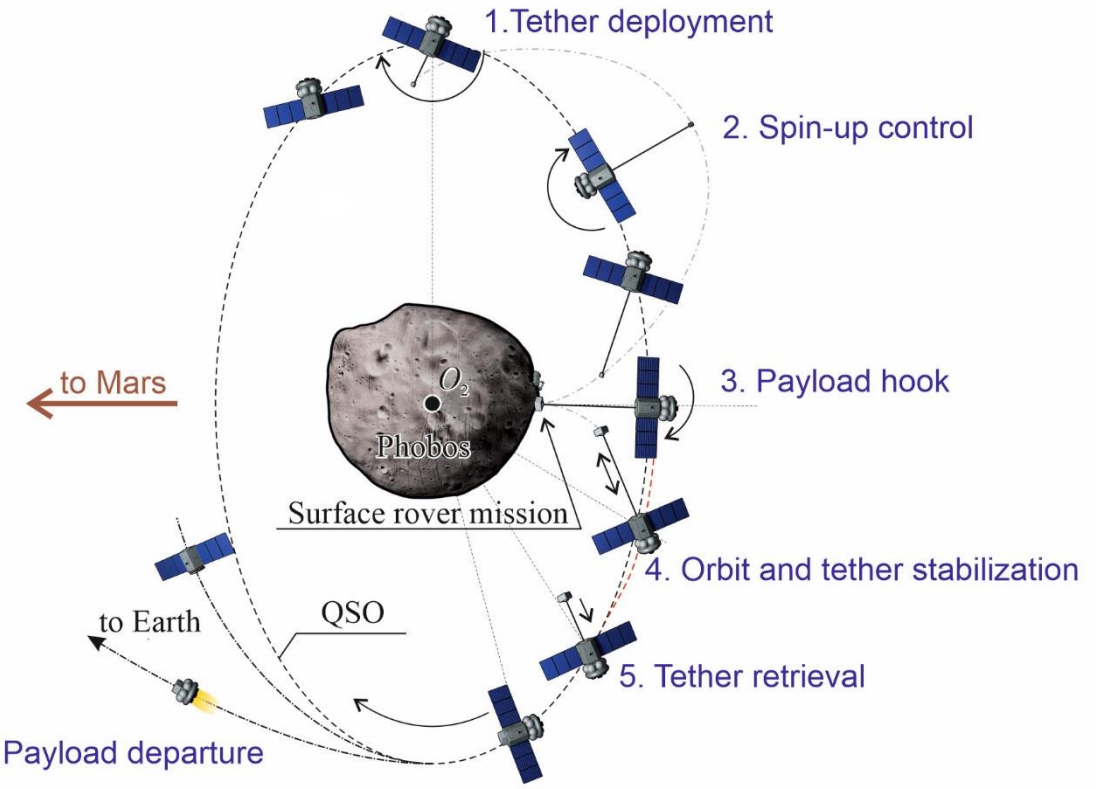


Fig. 3 – Phase of the collected soil lifting to the orbiter.

The described design is similar to the well-known skyhook concept. However, unlike the classical skyhook, the orbiter moves in a quasi-satellite orbit rather than a circular one, which requires additional control and synchronization. A key distinction is the need to compensate for the vertical component of velocity, because the orbiter itself may have such a component at the contact point with the surface owing to the non-circular orbit.

Table 1 - Mission Phase Stages

	Rover delivery phase	Container lifting phase	Description
№	Stage	Stage	
1	Tether deployment	Tether deployment	Deployment of the tether to its full length.

This is a **preprint** version of the article. It has not been peer reviewed. The definitive, peer-reviewed published version is:

Aslanov V.S., Ledkov A.S., Skyhook in Phobos's QSO: Preliminary design, tether deployment, and rover delivery, Acta Astronautica, Vol. 252, 2027, Pages 288–296, https://doi.org/10.1016/j.actaastro.2026.11.029.

2	Spin-up control	Spin-up control	Synchronisation of the orbital motion and rotation of the system about its centre of mass, ensuring zero relative velocity at the point of contact with the surface.
3	Payload release	Payload hook	Separation of the payload from the tether tip, or entanglement of the payload with the tether at the point of contact.
4	Orbit and tether stabilization	Orbit and tether stabilization	Counteraction of disturbances induced by abrupt changes in the mass at the tether tip.
5	Tether retrieval	Tether retrieval	Retraction of the tether into the orbiter, followed by transition to standby mode or preparation of the lifted container for Earth transfer.

3. Mathematical model

3.1. Equations of motion

The motion of a space tether system is considered under the conditions of the planar circular restricted three-body problem. Mars and Phobos move about their common centre of mass (point O in Fig 3) with an angular velocity n. The space tether system consists of two mass points, B_1 (orbiter) and B_2, connected by a massless rod of length l. The position of the system is described by four generalised coordinates: f is the angle of deviation of the line connecting the centres of mass of Mars and Phobos from the OX axis of the inertial coordinate system OXY; ρ is

This is a **preprint** version of the article. It has not been peer reviewed. The definitive, peer-reviewed published version is:

Aslanov V.S., Ledkov A.S., Skyhook in Phobos's QSO: Preliminary design, tether deployment, and rover delivery, Acta Astronautica, Vol. 252, 2027, Pages 288–296, https://doi.org/10.1016/j.actaastro.2026.11.029.

the distance from the centre of mass of Phobos, O_2, to the centre of mass of the tether system, C; φ is the angle of deviation of the vector $\mathbf{O_2C}$ from the line O_1O_2; and θ is the angle of deviation of the tether from the direction $\mathbf{O_2C}$. To derive the equations of motion, the Lagrange formalism is employed.

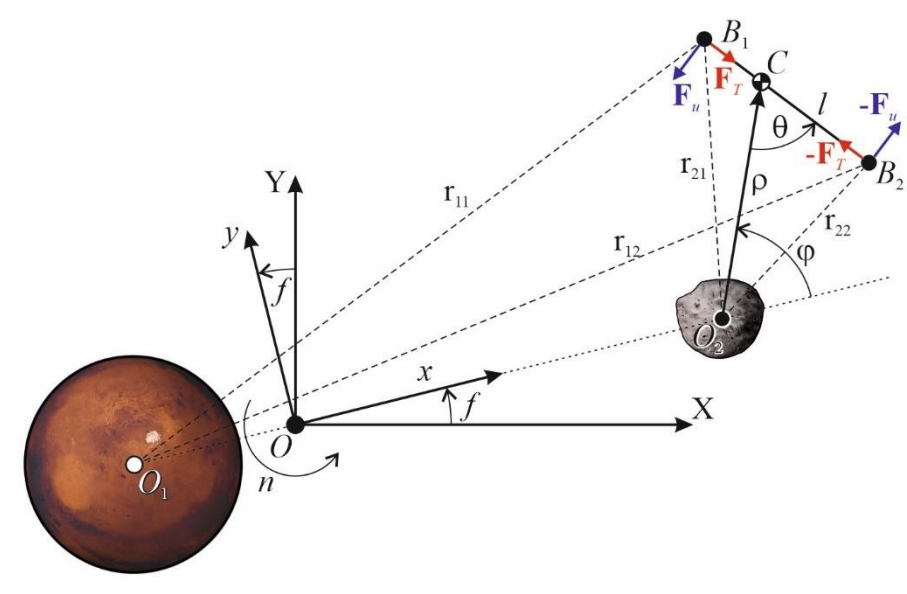


Fig. 3. Space tether system.

Prior to constructing the Lagrange function, some preliminary calculations are performed. The coordinates of the position vectors of points B_1 and B_2 are written in the inertial coordinate system OXY as

$$\begin{aligned}\mathbf{r}_{B1} &= \overrightarrow{OB_1} = [x_1\cos f - y_1\sin f, y_1\cos f + x_1\sin f]^T,\\ \mathbf{r}_{B2} &= \overrightarrow{OB_2} = [x_2\cos f - y_2\sin f, y_2\cos f + x_2\sin f]^T,\end{aligned} \tag{1}$$

where x_i and y_i are the coordinates of point B_i in the rotating frame Oxy, the axis Ox of which is aligned with the Mars-Phobos line and points towards Phobos. These coordinates are defined by the expressions

$$\begin{aligned}x_1 &= (1-\mu)r + \rho\cos\varphi + \bar{m}_2 l\cos(\theta+\varphi), \quad y_1 = \rho\sin\varphi + \bar{m}_2 l\sin(\theta+\varphi),\\ x_2 &= (1-\mu)r + \rho\cos\varphi - \bar{m}_1 l\cos(\theta+\varphi), \quad y_2 = \rho\sin\varphi - \bar{m}_1 l\sin(\theta+\varphi),\end{aligned} \tag{2}$$

This is a **preprint** version of the article. It has not been peer reviewed. The definitive, peer-reviewed published version is:

Aslanov V.S., Ledkov A.S., Skyhook in Phobos's QSO: Preliminary design, tether deployment, and rover delivery, Acta Astronautica, Vol. 252, 2027, Pages 288–296, https://doi.org/10.1016/j.actaastro.2026.11.029.

where $\mu = M_2 / (M_1 + M_2)$ is the mass ratio of the Mars-Phobos system, M_1 is the mass of Mars, M_2 is the mass of Phobos, r is the distance between the centers of mass of Mars and Phobos, $\bar{m}_i = m_1 / (m_1 + m_2)$ is the dimensionless mass, m_1 is the mass of the orbiter, m_2 is the mass of the tether tip (rover, container or just space hook). Vectors $\mathbf{r}_{ij}$, connecting points O_j with points B_i, have the following coordinates in the rotating reference frame Oxy

$$\begin{aligned}
\mathbf{r}_{11} &= \overrightarrow{O_1B_1} = [r + \rho\cos\varphi + \bar{m}_2 l\cos(\theta+\varphi),\ \rho\sin\varphi + \bar{m}_2 l\sin(\theta+\varphi)]^T,\\
\mathbf{r}_{12} &= \overrightarrow{O_1B_2} = [r + \rho\cos\varphi - \bar{m}_1 l\cos(\theta+\varphi),\ \rho\sin\varphi - \bar{m}_1 l\sin(\theta+\varphi)]^T,\\
\mathbf{r}_{21} &= \overrightarrow{O_2B_1} = [\rho\cos\varphi + \bar{m}_2 l\cos(\theta+\varphi),\ \rho\sin\varphi + \bar{m}_2 l\sin(\theta+\varphi)]^T,\\
\mathbf{r}_{22} &= \overrightarrow{O_2B_2} = [\rho\cos\varphi - \bar{m}_1 l\cos(\theta+\varphi),\ \rho\sin\varphi - \bar{m}_1 l\sin(\theta+\varphi)]^T.
\end{aligned} \tag{3}$$

Assuming the tether to be massless, the kinetic energy of the mechanical system takes the form

$$T = \frac{m_1 V_1^2}{2} + \frac{m_2 V_2^2}{2} = \sum_{i=1}^{2} \frac{m_i}{2}\left((\dot{x}_i - y_i\dot{f})^2 + (\dot{y}_i + x_i\dot{f})^2\right), \tag{4}$$

where V_i is the velocity of B_i point. The derivatives $\dot{x}_i$, and $\dot{y}_i$ are calculated taking into account (2). The potential energy of the system is

$$P = -\frac{GM_1m_1}{r_{11}} - \frac{GM_1m_2}{r_{12}} - \frac{GM_2m_1}{r_{21}} - \frac{GM_2m_2}{r_{22}}, \tag{5}$$

where G is Newtonian gravitational constant, r_{ij} is the length of the vectors (3). Using expressions (4) and (5), we construct the Lagrangian $L = T - P$ and then write the Lagrange equations of the second kind in the form

$$\frac{d}{dt}\frac{\partial L}{\partial \dot{q}_j} - \frac{\partial L}{\partial q_j} = Q_j, \tag{6}$$

where q_j is the generalized coordinate, Q_j is the corresponding generalized force

$$Q_j = \mathbf{F}_1 \cdot \frac{\partial \mathbf{r}_{B1}}{\partial q_j} + \mathbf{F}_2 \cdot \frac{\partial \mathbf{r}_{B2}}{\partial q_j}, \tag{7}$$

This is a **preprint** version of the article. It has not been peer reviewed. The definitive, peer-reviewed published version is:

Aslanov V.S., Ledkov A.S., Skyhook in Phobos's QSO: Preliminary design, tether deployment, and rover delivery, Acta Astronautica, Vol. 252, 2027, Pages 288–296, https://doi.org/10.1016/j.actaastro.2026.11.029.

where $\mathbf{F}_i$ is the resultant of non-potential forces applied to point B_i. The non-potential forces consist of the tether tension F_T and the thruster forces F_u; the latter are generated by oppositely directed thrusters mounted at the tether ends for spin-up control. The resultant force has the following coordinates in the inertial reference frame OXY

$$\begin{aligned}\mathbf{F}_1 &= [-F_T\cos\psi - F_u\sin\psi, -F_T\sin\psi + F_u\cos\psi]^T,\\ \mathbf{F}_2 &= [F_T\cos\psi + F_u\sin\psi,\ F_T\sin\psi - F_u\cos\psi]^T,\end{aligned} \tag{8}$$

where $\psi = f + \theta + \varphi$. Substituting (2) into (1) gives the following expressions for the generalized forces

$$Q_l = -F_T,\quad Q_\rho = 0,\quad Q_\varphi = F_u l,\quad Q_\theta = F_u l, \tag{9}$$

For the case of the restricted circular three-body problem

$$r = const,\ \dot{f} = \sqrt{G(M_1 + M_2)r^{-3}} = n. \tag{10}$$

Substituting (4), (5) and (9) into (6) and resolving the system with respect to the second derivatives yields the following equations of motion of the system

$$\ddot{\rho} = \rho(n+\dot{\varphi})^2 + n^2 r(1-\mu)\cos\varphi - \frac{1}{m_1+m_2}\frac{\partial P}{\partial \rho}, \tag{11}$$

$$\ddot{\varphi} = -\frac{2\dot{\rho}(n+\dot{\varphi})}{\rho} - \frac{n^2 r(1-\mu)\sin\varphi}{\rho} + \frac{1}{(m_1+m_2)\rho^2}\left(\frac{\partial P}{\partial \theta} - \frac{\partial P}{\partial \varphi}\right), \tag{12}$$

$$\ddot{l} = l(n+\dot{\varphi}+\dot{\theta})^2 - \frac{(m_1+m_2)}{m_1 m_2}\left(F_T + \frac{\partial P}{\partial l}\right), \tag{13}$$

$$\begin{aligned}\ddot{\theta} = {} & \frac{2\dot{\rho}(n+\dot{\varphi})}{\rho} + \frac{n^2 r(1-\mu)\sin\varphi}{\rho} - \frac{2\dot{l}(n+\dot{\varphi}+\dot{\theta})}{l} + \frac{1}{(m_1+m_2)\rho^2}\frac{\partial P}{\partial \varphi}\\ & - \left(\frac{1}{(m_1+m_2)\rho^2} + \frac{m_1+m_2}{m_1 m_2 l^2}\right)\frac{\partial P}{\partial \theta} + \frac{m_1+m_2}{m_1 m_2 l}F_u.\end{aligned} \tag{14}$$

where

This is a **preprint** version of the article. It has not been peer reviewed. The definitive, peer-reviewed published version is:

Aslanov V.S., Ledkov A.S., Skyhook in Phobos's QSO: Preliminary design, tether deployment, and rover delivery, Acta Astronautica, Vol. 252, 2027, Pages 288–296, https://doi.org/10.1016/j.actaastro.2026.11.029.

$$\frac{\partial P}{\partial \rho}=\frac{Gm_1m_2l\cos\theta}{m_1+m_2}\left(\frac{M_1}{r_{11}^3}-\frac{M_1}{r_{12}^3}+\frac{M_2}{r_{21}^3}-\frac{M_2}{r_{22}^3}\right)+GM_1r\cos\varphi\left(\frac{m_1}{r_{11}^3}+\frac{m_2}{r_{12}^3}\right)+G\rho\left(\frac{M_1m_1}{r_{11}^3}+\frac{M_1m_2}{r_{12}^3}+\frac{M_2m_1}{r_{21}^3}+\frac{M_2m_2}{r_{22}^3}\right), \tag{15}$$

$$\frac{\partial P}{\partial \varphi}=-\frac{Gm_1m_2M_1lr\sin(\theta+\varphi)}{m_1+m_2}\left(\frac{1}{r_{11}^3}-\frac{1}{r_{12}^3}\right)-GM_1r\rho\sin\varphi\left(\frac{m_1}{r_{11}^3}+\frac{m_2}{r_{12}^3}\right), \tag{16}$$

$$\frac{\partial P}{\partial l}=\frac{Gm_1m_2l}{(m_1+m_2)^2}\left(\frac{M_1m_2}{r_{11}^3}+\frac{M_1m_1}{r_{12}^3}+\frac{M_2m_2}{r_{21}^3}+\frac{M_2m_1}{r_{22}^3}\right)+\frac{Gm_1m_2M_1r\cos(\varphi+\theta)}{m_1+m_2}\left(\frac{1}{r_{11}^3}+\frac{1}{r_{12}^3}\right)+\frac{Gm_1m_2\rho\cos\theta}{m_1+m_2}\left(\frac{M_1}{r_{11}^3}-\frac{M_1}{r_{12}^3}+\frac{M_2}{r_{21}^3}-\frac{M_2}{r_{22}^3}\right), \tag{17}$$

$$\frac{\partial P}{\partial \theta}=-\frac{Gm_1m_2M_1lr\sin(\theta+\varphi)}{m_1+m_2}\left(\frac{1}{r_{11}^3}-\frac{1}{r_{12}^3}\right)-\frac{Gm_1m_2l\rho\sin\theta}{m_1+m_2}\left(\frac{M_1}{r_{11}^3}-\frac{M_1}{r_{12}^3}+\frac{M_2}{r_{21}^3}-\frac{M_2}{r_{22}^3}\right), \tag{18}$$

This system of equations describes the motion of a space tether system under the conditions of a restricted planar circular three-body problem. It differs from the formulation presented in [10] in the choice of generalised coordinates. Using the position vector of the centre of mass of the entire system rather than that of the orbiter allows the equations of motion to be derived in a more compact form.

3.2. Tether length control

The mission phases discussed in this paper require control of the tether system. The tether length is adjusted using a deployment mechanism installed on the orbiter. To model the deployment process, the tether length $l(t)$ is assumed to be a prescribed function. The motion of the system is then governed by equations (11), (12), and (14), while equation (13) provides the corresponding tether tension force.

$$F_T=\frac{m_1m_2}{m_1+m_2}\left((n+\dot\varphi+\dot\theta)^2l(t)-\ddot l(t)\right)-\frac{\partial P}{\partial l}. \tag{19}$$

This is a **preprint** version of the article. It has not been peer reviewed. The definitive, peer-reviewed published version is:

Aslanov V.S., Ledkov A.S., Skyhook in Phobos's QSO: Preliminary design, tether deployment, and rover delivery, Acta Astronautica, Vol. 252, 2027, Pages 288–296, https://doi.org/10.1016/j.actaastro.2026.11.029.

The tension must remain positive throughout the entire motion; otherwise, the tether sags, rendering the control law $l(t)$ physically unrealisable, as it would require the tether to act as a compressed spring pushing the attached bodies apart.

To implement tether deployment in this study, the following analytical law is proposed

$$l(t) = l_{\max} - (l_{\max} - l_0) e^{-\frac{V_0 t}{l_{\max} - l_0} - bt^2}. \tag{20}$$

where l_0 is the initial tether length, $l_{\max}$ is the final tether length, V_0 is the initial tether deployment speed, b is the coefficient influencing the rate of saturation of the law. At the initial stage of deployment, the tether length nearly linearly, but then its growth rate slows down, asymptotically approaching $l_{\max}$.

4. Numerical simulations

4.1. Parameters of the system

The present study is based on the MMX mission. The values of the constants used in the calculations are given in Table 2. The orbiter is assumed to have been delivered to a low quasi-satellite orbit. The distance from the center of Phobos to the nearest point in the orbit is 15000 m. Using equations (11) and (12) for a zero-length tether, the initial conditions that yield a periodic quasi-satellite orbit for the orbiter and the docked rover were identified through numerical search

$$\rho_0 = 15000\,\text{m},\ \dot{\rho}_0 = 0,\ \varphi_0 = 0,\ \dot{\varphi}_0 = -7.4364 \cdot 10^{-4}\,\text{rad/s}. \tag{21}$$

The contact point for rover deployment was chosen as the point on Phobos's surface closest to the selected quasi-satellite orbit. This choice, on the one hand, ensures the use of a minimal tether length and, on the other hand, eliminates the risk of the tether's lower end striking the surface during rotation. At this point [29], $\rho = 12950\,\text{m}$, $\varphi = 0$. The following relations must be satisfied to ensure that the lower end of the tether has zero velocity relative to the surface at the point of contact

This is a **preprint** version of the article. It has not been peer reviewed. The definitive, peer-reviewed published version is:

Aslanov V.S., Ledkov A.S., Skyhook in Phobos's QSO: Preliminary design, tether deployment, and rover delivery, Acta Astronautica, Vol. 252, 2027, Pages 288–296, https://doi.org/10.1016/j.actaastro.2026.11.029.

$$\theta = 0, \quad \dot{\theta} = \Omega = \frac{\dot{\varphi}(\rho - \bar{m}_1 l)}{\bar{m}_1 l} \ . \tag{22}$$

Table 2 Parameters of the system

Parameter	Value
Mass of the Phobos[30]	$1.06597 \cdot 10^{16}$ kg
Mass of the Mars	$6.4169 \cdot 10^{23}$ kg
Phobos ellipsoid radii [29]	12950m × 11300m × 9160m
Mass of the orbiter	2800 kg
Mass of the rover	200 kg

4.2. Skyhook concept feasibility: rover delivery phase

To demonstrate the feasibility of the Skyhook concept under the circular restricted three-body problem, the transport operation for delivering a rover from a quasi-satellite orbit to the surface of Phobos is simulated. The timing of each stage is determined through a series of numerical experiments. Using successive approximations, the parameters of the initial orbit and the deployment duration are selected to ensure that the lower end of the tether touches the Phobos surface at the contact point with zero relative velocity. The deployment stage is assumed to start at the initial time. The resulting trajectory is not optimal in any sense; it merely serves to illustrate the feasibility of delivering the rover to the contact point with zero velocity relative to the surface.

The tether deployment phase begins at the point with coordinates $\rho = 15000\,\text{m}$, $\varphi = 0$. The tether is released in the direction of Phobos ($\theta_0 = 0$). Equations (11), (12), and (14) are used to simulate the system motion at this stage. The tether length is determined by law (20). Equation (19) is used to control the tension force. This force must remain positive throughout the manoeuvre. Based on the orbiter's orbital geometry, the tether length was chosen so that, at the moment of crossing the Mars-Phobos line, the distance from the system's centre of mass to the

This is a **preprint** version of the article. It has not been peer reviewed. The definitive, peer-reviewed published version is:

Aslanov V.S., Ledkov A.S., Skyhook in Phobos's QSO: Preliminary design, tether deployment, and rover delivery, Acta Astronautica, Vol. 252, 2027, Pages 288–296, https://doi.org/10.1016/j.actaastro.2026.11.029.

contact point matches the tether length from the centre of mass to the rover attachment point at the tether's end CB_2 (Fig. 3). In this case

$$l_2 = CB_2 = 2050\,\text{m},\ l_1 = CB_1 = 146.43\,\text{m},\ l_{\max} = l_1 + l_2 = 2196.43\,\text{m} \qquad (23)$$

The initial tether length was chosen as $l_0 = 0.1\,\text{m}$. The parameter V_0 determines the tether release velocity. For the considered initial conditions, numerical simulations showed that at release velocities below approximately 3 m/s, the tether sags during the initial stage. The initial velocity was set to $V_0 = 3.2\,\text{m/s}$. The parameter b affects the deceleration rate of deployment. Is was chosen as $b = 10^{-6}\,\text{s}^{-2}$. With the selected values, deployment of the tether to within 1 mm of its final length takes 3162 s. Fig. 4 shows the tether length as a function of time for different parameter sets, and the corresponding tension forces are presented in Fig. 5. The black line corresponds to the option selected for further simulation.

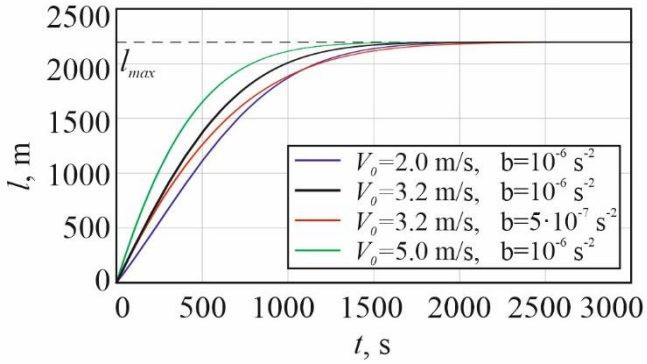


Fig. 4. Dependence of the tether length controlled by law (20) on time for different sets of control parameters.

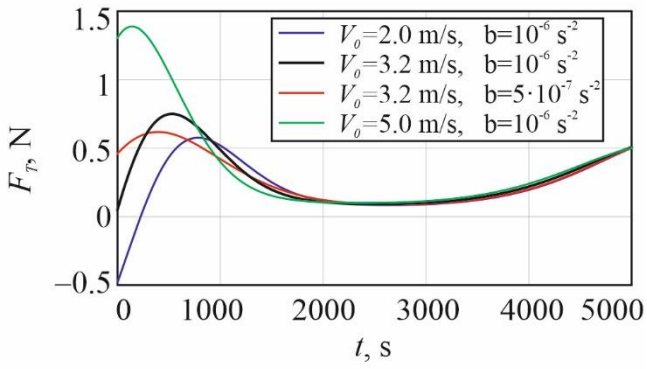


Fig. 5. Dependence of the tension force on time for different sets of control parameters.

This is a **preprint** version of the article. It has not been peer reviewed. The definitive, peer-reviewed published version is:

Aslanov V.S., Ledkov A.S., Skyhook in Phobos's QSO: Preliminary design, tether deployment, and rover delivery, Acta Astronautica, Vol. 252, 2027, Pages 288–296, https://doi.org/10.1016/j.actaastro.2026.11.029.

After deployment, the tether system enters a mode of relatively large-amplitude oscillations (Fig. 6). Conversion to rotational motion can be achieved, for example, using a pair of oppositely directed thrusters, each generating a constant force $F_u = 10\,\mathrm{N}$. The operating time of the thrusters is selected in such a way that the angular velocity module of the tether system $\dot{\theta}$ increases to the value Ω given by (22). The thrusters are activated at a time chosen such that, when the tether system crosses $\varphi = 0$, the tether is aligned with the local vertical, that is, $\theta = 0$. If, at this point, the distance between the lower end of the tether system and the surface of Phobos is greater than zero, the initial conditions are modified by increasing the height ρ_0. Otherwise, the initial conditions are decreased. For this new altitude, the initial angular velocity is selected so that the orbit is closed, and the calculations are repeated.

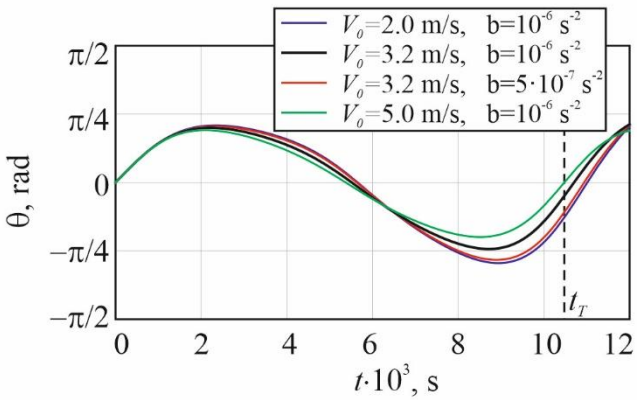


Fig. 6. Dependence of the tether deflection angle on time for different sets of control parameters.

After several iterations, the following initial conditions and time instants were obtained.

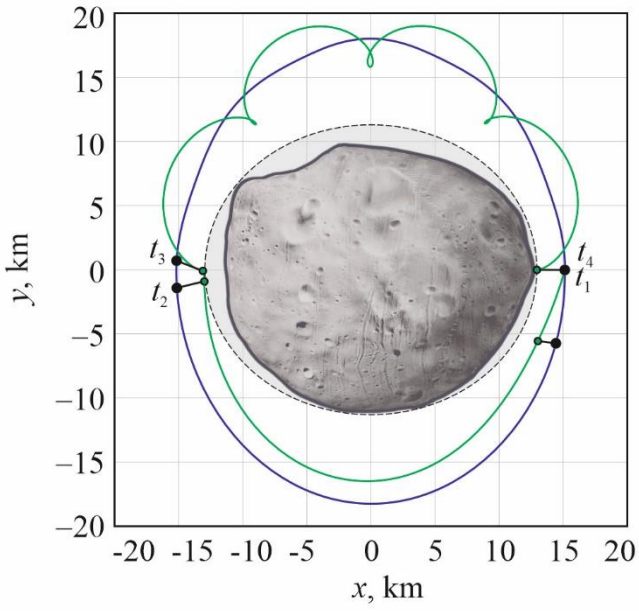
$$\rho_0 = 15123.50\,\mathrm{m},\ \dot{\rho}_0 = 0,\ \varphi_0 = 0,\ \dot{\varphi}_0 = -7.3859\cdot 10^{-4}\,\mathrm{rad/s},\qquad (24)$$

$$t_1 = 0\,\mathrm{s},\ t_2 = 5155\,\mathrm{s},\ t_3 = 5335\,\mathrm{s},\ t_4 = 10480\,\mathrm{s}\qquad (25)$$

This is a **preprint** version of the article. It has not been peer reviewed. The definitive, peer-reviewed published version is:

Aslanov V.S., Ledkov A.S., Skyhook in Phobos's QSO: Preliminary design, tether deployment, and rover delivery, Acta Astronautica, Vol. 252, 2027, Pages 288–296, https://doi.org/10.1016/j.actaastro.2026.11.029.

where t_1 is the start time of deployment, t_2 is the time of the thrusters activation to deploy the tether system, t_3 is the thrusters shutdown time, t_4 is the time of rover contact with the surface and its detachment from the tether. Fig. 7 shows the trajectory of the rover (green line) and orbiter (blue line) during the maneuver in question. The figure also shows the positions of the tether system at the indicated times. The distances from the center of Phobos to the orbiter (r_{21}), rover (r_{22}), center of mass of the system ρ, and surface of the Phobos are shown in Fig. 8. As can be seen from Figs. 7 and 8, the rover approaches Phobos's surface at a relatively close distance at approximately 5250 s. The minimum distance between Phobos's surface and the rover exceeds 35 m. The rover's velocity relative to the surface at this point is approximately 2.5 m/s. Fig. 9 shows the rover's velocity relative to the surface as a function of time. It can be seen that at the point of contact at time t_4 the relative velocity of the rover is zero. The tether tension remains positive throughout the maneuver. The tension does not exceed 12N, which is easily achievable in practice (Fig. 10). The dependence of angular velocity on time is demonstrated in Fig. 11. Turning on two thrusters for three minutes allows increasing the angular velocity of the tether system to the required value Ω, which is determined by expression (22).



This is a **preprint** version of the article. It has not been peer reviewed. The definitive, peer-reviewed published version is:

Aslanov V.S., Ledkov A.S., Skyhook in Phobos's QSO: Preliminary design, tether deployment, and rover delivery, Acta Astronautica, Vol. 252, 2027, Pages 288–296, https://doi.org/10.1016/j.actaastro.2026.11.029.

Fig. 7. The trajectory of the orbiter (blue line) and the rover (green line) connected by a tether.

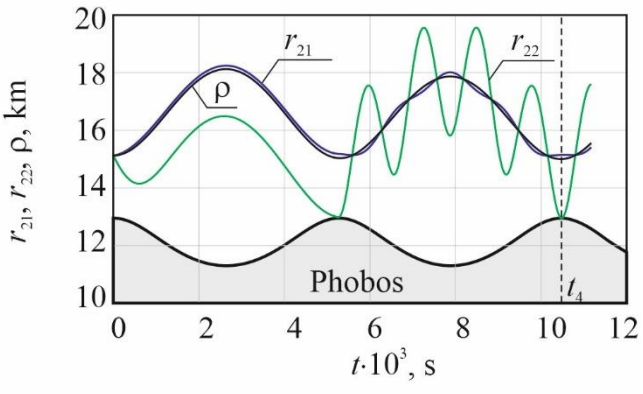


Fig. 8. Changes in distances from points in the system to the center of Phobos over time.

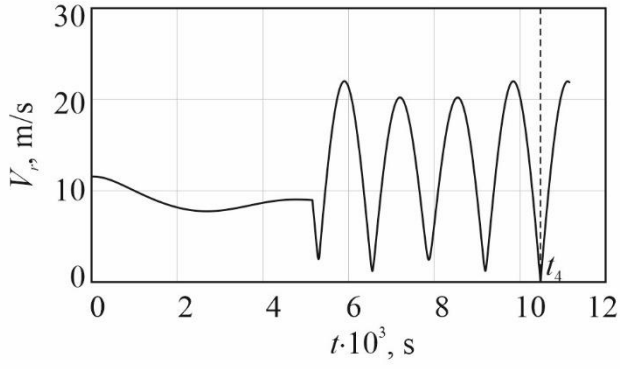


Fig. 9. The rover's speed relative to the surface of Phobos.

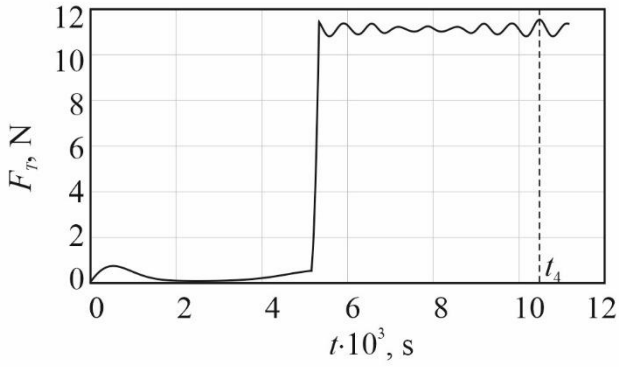


Fig. 10. Dependence of the tension force of the rope on time.

This is a **preprint** version of the article. It has not been peer reviewed. The definitive, peer-reviewed published version is:

Aslanov V.S., Ledkov A.S., Skyhook in Phobos's QSO: Preliminary design, tether deployment, and rover delivery, Acta Astronautica, Vol. 252, 2027, Pages 288–296, https://doi.org/10.1016/j.actaastro.2026.11.029.

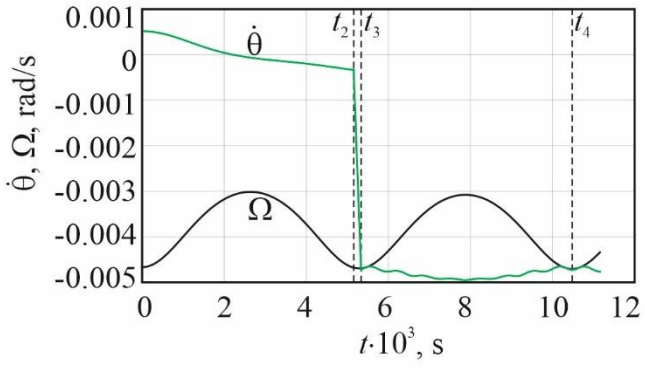


Fig. 11. Dependence of the angular velocity of rotation of the tether on time.

The results of numerical simulations confirm the possibility of using the scheme proposed by Skyhook for delivering a rover from a quasi-satellite orbit to the surface of Phobos.

4.3. Deploying the tether from rotation mode.

Spinning up the space tether system is an important part of the Skyhook concept considered in this work. In the previous subsection, a solution to this problem was proposed using two thrusters that create a force couple accelerating the tether system to the desired angular velocity. In this section, an alternative concept is considered, in which deployment occurs directly from the rotation mode. In this case, the orbiter is spun up before the tether is released. The initial angular rate $\dot{\theta}_0$ is selected so that, using the tether length control law (20), the angular velocity at the end of deployment corresponds to (22). This initial angular velocity must significantly exceed the required angular velocity Ω, since, in the absence of external torques, the angular momentum relative to the system's center of mass is conserved, and the increase in the moment of inertia during tether deployment is compensated by a decrease in angular velocity.

To achieve a final angular velocity of $\dot{\theta} = \Omega$, the initial angular velocity was set to $\dot{\theta}_0 = -2.521 \cdot 10^6 \text{s}^{-1}$. Fig. 12 shows the time history of the angular velocity. The trajectories of the orbiter and the rover, connected by the tether, are presented

This is a **preprint** version of the article. It has not been peer reviewed. The definitive, peer-reviewed published version is:

Aslanov V.S., Ledkov A.S., Skyhook in Phobos's QSO: Preliminary design, tether deployment, and rover delivery, Acta Astronautica, Vol. 252, 2027, Pages 288–296, https://doi.org/10.1016/j.actaastro.2026.11.029.

in Fig. 13. This preliminary calculation indicates that, theoretically, spin-up from the rotation mode enables a rover delivery mission from a quasi-satellite orbit to the Phobos surface; however, the required initial spin-up velocity exceeds the limits of physical feasibility.

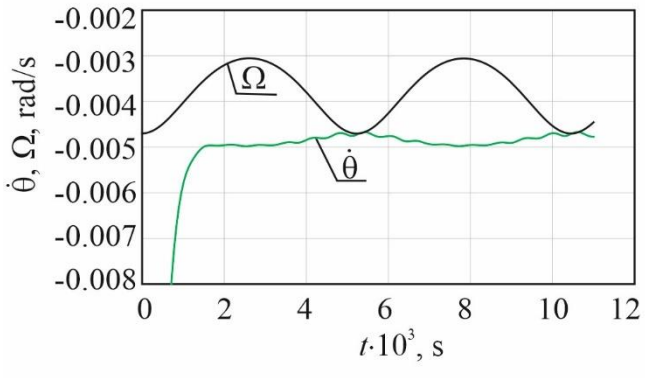


Fig. 12. Dependence of the angular velocity of rotation of the tether on time for the case deployment from rotation mode.

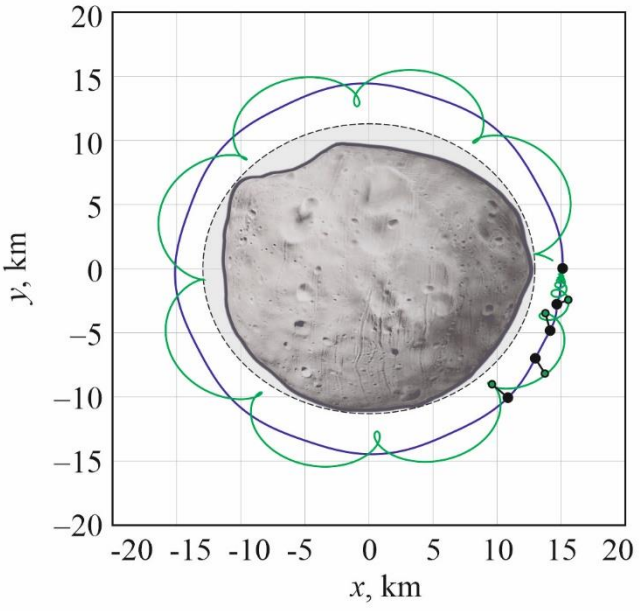


Fig. 13. The trajectory of the orbiter (blue line) and the rover (green line) connected by a tether in the case of the tether deployment in rotation mode.

6. Conclusion

This is a **preprint** version of the article. It has not been peer reviewed. The definitive, peer-reviewed published version is:

Aslanov V.S., Ledkov A.S., Skyhook in Phobos's QSO: Preliminary design, tether deployment, and rover delivery, Acta Astronautica, Vol. 252, 2027, Pages 288–296, https://doi.org/10.1016/j.actaastro.2026.11.029.

This article examines the physical feasibility of a mission to deliver a rover from a low quasi-satellite orbit to the surface of Phobos using a rotating tether system. The design is based on the Skyhook concept, which utilises the rotation of the tether system to achieve zero relative velocity with respect to the surface at the moment the payload detaches from the tether at its lowest point. Unlike the classical design, the centre of mass of the tether system moves in a quasi-satellite orbit under the restricted three-body problem, and the target surface is non-spherical.

The main results of the paper are as follows:

1. A concept for a Phobos exploration mission using a variable-length rotating tether system is formulated, and its principal phases are described.
2. A simplified mathematical model describing the motion of the tether system under the circular restricted three-body problem is developed.
3. An analytical law describing the deployment of the tether system is proposed. This law differs from classical exponential deployment laws by the presence of a quadratic term in the exponent, which affects the rate of approach to the full tether length.
4. Numerical simulations confirming the feasibility of payload delivery from a low quasi-satellite orbit to the Phobos surface using the Skyhook idea are conducted. A pair of thrusters is used to spin up the tether system.
5. It is shown that pre-spinning the orbiter before tether deployment to achieve the required angular velocity would demand an impractically large initial angular velocity and is therefore not feasible in practice.

The assumptions adopted in this study, including planar motion, massless tether, orbiter and rover treated as point masses, circular restricted three-body problem, are sufficient to verify the fundamental feasibility of the Skyhook concept for non-Keplerian orbits. A more detailed mission analysis, including the selection of optimal operating modes, the development of control laws for the tether and thrusters, and an assessment of their robustness, will require more accurate

mathematical models and a deeper numerical investigation. These aspects are beyond the scope of the present work and are therefore deferred to future studies.

Acknowledgments

The study was supported by a grant from the Russian Science Foundation № 26-19-00260, https://rscf.ru/project/26-19-00260/.

References

[1] T. Usui, K. Bajo, W. Fujiya, Y. Furukawa, M. Koike, Y.N. Miura, H. Sugahara, S. Tachibana, Y. Takano, K. Kuramoto, The Importance of Phobos Sample Return for Understanding the Mars-Moon System, Space Sci. Rev. 216 (2020) 49. https://doi.org/10.1007/s11214-020-00668-9.

[2] R.Z. Sagdeev, A. V Zakharov, Brief history of the Phobos mission, Nature. 341 (1989) 581–585. https://doi.org/10.1038/341581a0.

[3] A.L. Albee, R.E. Arvidson, F. Palluconi, T. Thorpe, Overview of the Mars Global Surveyor mission, J. Geophys. Res. Planets. 106 (2001) 23291–23316. https://doi.org/10.1029/2000JE001306.

[4] P. Martin, D. Titov, C. Wilson, A. Cardesín-Moinelo, J. Godfrey, J.P. Bibring, F. González-Galindo, R. Jaumann, A. Määttänen, T. Spohn, G. Kminek, E. Sefton-Nash, Mars Express: From the Launch Pad to a 20-Year Success Record at Mars, Space Sci. Rev. 221 (2025). https://doi.org/10.1007/s11214-025-01174-6.

[5] J.E. Graf, R.W. Zurek, H.J. Eisen, B. Jai, M.D. Johnston, R. DePaula, The Mars Reconnaissance Orbiter Mission, Acta Astronaut. 57 (2005) 566–578. https://doi.org/10.1016/j.actaastro.2005.03.043.

[6] M.Y. Marov, V.S. Avduevsky, E.L. Akim, T.M. Eneev, R.S. Kremnev, S.D. Kulikov, K.M. Pichkhadze, G.A. Popov, G.N. Rogovsky, Phobos-Grunt: Russian sample return mission, Adv. Sp. Res. 33 (2004) 2276–2280. https://doi.org/10.1016/S0273-1177(03)00515-5.

[7] Y. Kawakatsu, K. Kuramoto, T. Usui, H. Sugahara, H. Ootake, R. Yasumitsu, K. Yoshikawa, S. Mary, M. Grebenstein, H. Sawada, T. Imada, T. Shimada, K. Ogawa, M. Otsuki, M. Baba, K. Fujita, K. Zacny, D. van Dyne, Y. Satoh, A. Tokaji, Preliminary design of Martian Moons eXploration (MMX), Acta Astronaut. 202 (2023) 715–728. https://doi.org/10.1016/j.actaastro.2022.09.009.

[8] P. Lee, J. Veverka, J. Bellerose, Hall: a Phobos and Deimos sample return mission, in: 41st Annu. Lunar Planet. Sci. Conf., The Woodlands, Texas, USA, 2010: p. 1633.

[9] K. Kempton, J. Pearson, E. Levine, J. Carroll, F. Amzajerdian, Phase 1 Study for the Phobos L1 Operational Tether Experiment (PHLOTE), 2018.

[10] V.S. Aslanov, Tether System in Martian-Moons-eXploration-Like Mission for Phobos Surface Exploration, J. Spacecr. Rockets. 61 (2024) 319–326. https://doi.org/10.2514/1.A35777.

[11] V.S. Aslanov, A space elevator deployed at the L1 Mars–Phobos libration point, Nonlinear Dyn. 112 (2024) 1–11. https://doi.org/10.1007/s11071-024-09762-x.

[12] V.S. Aslanov, A.S. Ledkov, Survey of Tether System Technology for Space Debris Removal Missions, J. Spacecr. Rockets. 60 (2023) 1355–1371. https://doi.org/10.2514/1.A35646.

[13] S.S. Afonso, M.P. Cartmell, Application of Symmetrical Motorised Momentum Exchange Tethers for Two-Way Earth–Mars Transportation, Sp. Sci. Technol. 5 (2025) 1–20. https://doi.org/10.34133/space.0325.

[14] H. Kojima, P.M. Trivailo, Model predictive tether-deployment control for precise landing of tethered reentry body, Adv. Sp. Res. 64 (2019) 1537–1548. https://doi.org/10.1016/j.asr.2019.07.025.

[15] F. Zimmermann, U.M. Schöttle, E. Messerschmid, Optimization of the tether-assisted return mission of a guided re-entry capsule, Aerosp. Sci. Technol. 9 (2005) 713–721. https://doi.org/10.1016/j.ast.2005.09.002.

[16] L. Perek, Space Elevator: Stability, Acta Astronaut. 62 (2008) 514–520. https://doi.org/10.1016/j.actaastro.2008.01.020.

[17] V.S. Aslanov, An anchored space elevator under the L1 Mars-Phobos libration point, Acta Astronaut. 235 (2025) 38–46. https://doi.org/10.1016/j.actaastro.2025.05.032.

[18] P. Jerome, L. Eugene, O. John, W. Harry, The Lunar Space Elevator, in: 55th Int. Astronaut. Congr. Int. Astronaut. Fed. Int. Acad. Astronaut. Int. Inst. Sp. Law, American Institute of Aeronautics and Astronautics, Reston, Virigina, 2004: pp. 1–11. https://doi.org/10.2514/6.IAC-04-IAA.3.8.3.07.

[19] J. Huang, A.K. Misra, Controlled deployment of a long tether to operate as a partial space elevator, Astrodynamics. 8 (2024) 311–321. https://doi.org/10.1007/s42064-024-0225-5.

[20] G. Shi, Z.H. Zhu, New geometric formulation for libration dynamics and suppression of partial space elevator by fuzzy logic and thrust vectoring control, Acta Astronaut. 217 (2024) 293–301. https://doi.org/10.1016/j.actaastro.2024.02.005.

[21] H. Jiang, R. Zhong, R. Qi, Electrodynamic tether and brake sails combination deorbit design, Acta Astronaut. 226 (2025) 669–678. https://doi.org/10.1016/j.actaastro.2024.11.007.

[22] A. Valmorbida, L. Olivieri, A. Brunello, G. Sarego, G. Sánchez-Arriaga, E.C. Lorenzini, Validation of enabling technologies for deorbiting devices based on electrodynamic tethers, Acta Astronaut. 198 (2022) 707–719. https://doi.org/10.1016/j.actaastro.2022.06.013.

[23] F. Yao, Q. Zhang, Z.H. Zhu, Near-surface lunar observation by tethered orbital platform for high-resolution long-duration exploration, Acta Astronaut. 246 (2026) 778–783. https://doi.org/10.1016/j.actaastro.2026.04.047.

[24] C. Bombardelli, J. Pelaez, E. Lorenzini, D. Curreli, M. Sanjurjo-Rivo, F. Lucas, D. Scheeres, M. Lara, Io Exploration with Electrodynamic Tethers, in:

This is a **preprint** version of the article. It has not been peer reviewed. The definitive, peer-reviewed published version is:

Aslanov V.S., Ledkov A.S., Skyhook in Phobos's QSO: Preliminary design, tether deployment, and rover delivery, Acta Astronautica, Vol. 252, 2027, Pages 288–296, https://doi.org/10.1016/j.actaastro.2026.11.029.

AIAA/AAS Astrodyn. Spec. Conf. Exhib., American Institute of Aeronautics and Astronautics, Reston, Virigina, 2008. https://doi.org/10.2514/6.2008-7384.

[25] H. Moravec, A non-synchronous orbital skyhook, J. Astronaut. Sci. 25 (1977) 307–322.

[26] J.D. Isaacs, A.C. Vine, H. Bradner, G.E. Bachus, Satellite Elongation into a True "Sky-Hook," Science (80-.). 151 (1966) 682–683. https://doi.org/10.1126/science.151.3711.682.

[27] M. Landgraf, T. Kavu, D.M. Jöckel, A multi-stage orbital sky hook for exploration in the new space transportation era, Acta Astronaut. 236 (2025) 1327–1336. https://doi.org/10.1016/j.actaastro.2025.07.018.

[28] R.P. Hoyt, C. Uphoff, Cislunar Tether Transport System, J. Spacecr. Rockets. 37 (2000) 177–186. https://doi.org/10.2514/2.3564.

[29] C.M. Ernst, R.T. Daly, R.W. Gaskell, O.S. Barnouin, H. Nair, B.A. Hyatt, M.M. Al Asad, K.K.W. Hoch, High-resolution shape models of Phobos and Deimos from stereophotoclinometry, Earth, Planets Sp. 75 (2023). https://doi.org/10.1186/s40623-023-01814-7.

[30] M. Pätzold, T. Andert, R. Jacobson, P. Rosenblatt, V. Dehant, Phobos: Observed bulk properties, Planet. Space Sci. 102 (2014) 86–94. https://doi.org/10.1016/j.pss.2014.01.004.